POLITECNICO DI TORINO
Repository ISTITUZIONALE

A free vibration analysis of three-dimensional sandwich beams using hierarchical one-dimensional finite elements

(Article begins on next page)

03 June 2024

A free vibration analysis of three-dimensional sandwich beams using hierarchical one-dimensional finite elements

Y. Hui[*],
Luxembourg Institute of Science and Technology,
5, avenue des Hauts-Fourneaux, L-4362 Esch-sur-Alzette, Luxembourg and
Politecnico di Torino, c.so Duca degli Abruzzi 24, 10129 Turin, Italy and
School of Civil Engineering, Wuhan University,
8 South Road of East Lake, 430072 Wuhan, PR China

G. Giunta[†],
Luxembourg Institute of Science and Technology,
5, avenue des Hauts-Fourneaux, L-4362 Esch-sur-Alzette, Luxembourg

S. Belouettar[‡],
Luxembourg Institute of Science and Technology,
5, avenue des Hauts-Fourneaux, L-4362 Esch-sur-Alzette, Luxembourg

Q. Huang[§],
School of Civil Engineering, Wuhan University,
8 South Road of East Lake, 430072 Wuhan, PR China

H. Hu[¶],
School of Civil Engineering, Wuhan University,
8 South Road of East Lake, 430072 Wuhan, PR China

E. Carrera[‖],
Politecnico di Torino, c.so Duca degli Abruzzi 24, 10129 Turin, Italy

Author for correspondence:
Yanchuan Hui, Ph.D. student,
Materials Research and Technology Department,
Luxembourg Institute of Science and Technology,
5, avenue des Hauts-Fourneaux,
L-4362 Esch-sur-Alzette, Luxembourg.
tel: +352 275 888 1,
fax: +352 275 885,
e-mail: yanchuan.hui@list.lu

---

[*]Ph.D. student.
[†]Research scientist.
[‡]Research scientist.
[§]Ph.D. student.
[¶]Full Professor.
[‖]Full Professor.

Abstract

This paper presents a family of beam higher-orders finite elements based on a hierarchical one-dimensional unified formulation for a free vibration analysis of three-dimensional sandwich structures. The element stiffness and mass matrices are derived in a nucleal form that corresponds to a generic term in the displacement field approximation over the cross-section. This fundamental nucleus does not depend upon the approximation order nor the number of nodes per element that are free parameters of the formulation. Higher-order beam theories are, then, obtained straightforwardly. Timoshenko's classical beam theory is obtained as a special case. Short and slender beams are investigated. Simply supported, cantilevered and clamped-clamped boundary conditions are considered. Several natural frequencies as well as the corresponding modes are investigated. Results are validated in terms of accuracy and computational costs towards three-dimensional finite element solutions. The proposed hierarchical models, upon an appropriate choice of approximation order, yield accurate results with a reduced computational cost.

Keywords: Free vibration analysis; Sandwich beam structures; Unified formulation; Finite element method.

1 Introduction

Sandwich beams are composed by a thick soft core and two thin stiff face sheets. They are widely used in several engineering sectors such as aeronautics and astronautics due to their high specific strength- and stiffness-to-weight ratios. Sandwich structures analysis and design was first discussed by Allen [1]. Many investigations were, then, devoted to static and dynamic analyses of these structures and various representative theories were proposed: classical laminate theory, first-order shear deformation theory and high-order theories as well as zig-zag based models. Some reviews of the theories for modelling sandwich structures can be found in Carrera [2] and Hu et al. [3].

Ahmed [4] used finite element displacement method to investigate the free vibration characteristics of curved sandwich beams under clamped-clamped boundary conditions. Goyal [5] studied the free vibrations of sandwich beams having a central mass. Shu [6] solved the free vibrations of sandwich beams with single and double delaminations analytically. Frostig and Baruch [7] presented a free vibration analysis of sandwich beams under simply supported boundary conditions based on a higher-order beam theory for the skins and a two-dimensional elasticity solution for the core. By applying the discrete Green function, a free vibration analysis of a three-layer sandwich beam with an elastic or viscoelatic core and arbitrary boundary conditions was presented by Sakiyama et al. [8]. Furthermore, a related work about continuous sandwich beams with elastic or viscoelastic cores was presented in [9]. Kameswara Rao et al. [10] used a fully third-order model of laminated composite and sandwich beams based on a higher-order mixed theory. Daya et al. [11] developed a new numerical method for an exact solution of non-linear eigenvalue problems that can be applied to determine the natural frequencies and the loss factors of viscoelastic damped sandwich structures. Banerjee [12] analysed the free vibration of three-layered symmetric sandwich beams using the Wittrick–Williams algorithm. By using the same method, Banerjee et al. [13] developed a dynamic stiffness theory of a three-layered sandwich beams. Kapuria et al. [14] presented a third-order zig-zag theory for the static, free and forced vibration analysis of sandwich beams. Bhangale and Ganesan [15] studied the buckling and vibration behaviour of a functionally graded material sandwich beam having constrained viscoelastic layer in thermal environment by using the finite element method. An assessment of higher-order and zig-zag displacement-based theories for the stability and free vibration of sandwich beams was proposed by Wu and Chen [16]. The element free Galerkin method and Galerkin formulation for two-dimensional elasticity problem were considered for the free vibration analysis of sandwich beams with a core made of a functionally graded material by Amirani et al. [17]. Arvin et al. [18] developed a model to study the free and forced vibration of composite sandwich viscoelastic-core beam based on a modified Mead-Markus theory. Vidal and Polit [19] presented a family of sinus models for the analysis of laminated beams in the framework of a free vibration analysis. Damanpack and Khalili [20] examined the high-order free vibration of three-layered symmetric sandwich beams using a dynamic stiffness method. An analytical solution for free vibration analysis of lattice sandwich beams was carried out by Lou et al. [21]. The lattice sandwich beam was transformed to an equivalent homogeneous three-layered sandwich beam. The natural frequencies of composite sandwich beams with lattice truss core were investigated by combining the classical Euler-Bernoulli beam theory and Timoshenko beam theory by Xu et al. [22]. Yang et al. [23] studied the free vibrations of functionally graded sandwich beams by a mesh-free boundary-domain integral equation method. Qu et al. [24] presented a three-dimensional free vibration

analysis of composite structures with parallelepiped shapes including beams, plates and solids. He et al. [25] investigated the free vibrations and buckling of composite beams by modifying Reddy's higher-order beam theory. Jin et al. [26] proposed a theoretical model using Reddy's higher-order shear deformation theory to analyse the vibration and damping of sandwich beams with a viscoelastic core. A free vibration analysis of asymmetric sandwich beams resting on a variable Pasternak foundation was carried out through Hamilton's principle and generalised Galerkin's method by Pradhan et al. [28]. A higher-order theory was developed to study the free vibrations of a debonded curved sandwich beam by Sadeghpour et al. [29]. Tossapanon and Wattanasakulpong [30] analysed the free vibrations of functionally graded sandwich beams resting on Winkler and shear layer springs based on Timoshenko's beam theory.

This paper presents a free vibration analysis of sandwich beams by several higher-order beam one-dimensional finite elements derived through a Unified Formulation (UF). This formulation has been previously applied for plates and shells (see Carrera [31], Carrera and Giunta [32] and Giunta et al. [33]) and lately extended to beams, see Carrera et al. [34, 35] and Giunta et al [36, 37, 38]. The hierarchical beam elements were extended to sandwich structures accounting for a layer-wise description of the displacement field by He et al. [39].

A study on three-dimensional nano-beams accounting for surface free energy effect were carried out in Giunta et al. [42]. The free vibration analysis of laminate composite beams was discussed in Giunta et al. [40]. A free vibration and a stability analysis of sandwich beams via Navier-type closed form solution was presented in Giunta et al. [41]. The present work is an extension of these previous works by using a finite element solution to investigate the free vibrations under different boundary conditions and to test the accuracy of the proposed models within the framework of a weak form solution. The elements stiffness and mass matrices are obtained via the Principle of Virtual Displacements (PVD). Through a concise notation for the displacement field, these matrices can be rewritten in a 'nucleal' form that does not depend upon the approximation order nor the number of nodes per element. Non-classical deformations, such as transverse shear and cross-section in- and out-of-plane warping, can have a significant influence on the response of beams, see Bishop et al. [43]. By using this formulation, classical theories can be easily enhanced in order to account for transverse shear, cross-section in- and out-of-plane warping and rotatory inertia. Classical Timoshenko's (TBT) model is obtained as a special case.

Results of these models are validated through comparison with three-dimensional finite element method solutions obtained via Ansys. Numerical results show that, upon a suitable choice of the expansion order for the displacement-based beam theory, accurate results can be obtained with reduced computational costs.

2 Preliminaries

A beam, see Fig. 1, is a structure whose axial extension (l) is higher than any other dimension orthogonal to it. The cross-section (Ω) is obtained by intersecting the beam with planes that are orthogonal to its axis. Equations are written in a Cartesian reference system: y- and z-axis are two orthogonal directions laying on Ω. The x coordinate is coincident with the beam axis. It is bounded such that $0 \leq x \leq l$. The cross-section is considered to be constant along x. The displacement field is:

$$\mathbf{u}^T (x, y, z) = \left\{ \begin{array}{ccc} u_x (x, y, z) & u_y (x, y, z) & u_z (x, y, z) \end{array} \right\} \tag{1}$$

in which u_x, u_y and u_z are the displacement components along x-, y- and z-axis, respectively. The transposition operator is represented by superscript 'T'. Stress, $\boldsymbol{\sigma}$, and strain, $\boldsymbol{\varepsilon}$, vectors are arranged into vectors $\boldsymbol{\sigma}_n$, $\boldsymbol{\varepsilon}_n$ on the cross-section:

$$\boldsymbol{\sigma}_n^T = \left\{ \begin{array}{ccc} \sigma_{xx} & \sigma_{xy} & \sigma_{xz} \end{array} \right\} \quad \boldsymbol{\varepsilon}_n^T = \left\{ \begin{array}{ccc} \varepsilon_{xx} & \varepsilon_{xy} & \varepsilon_{xz} \end{array} \right\} \tag{2}$$

and $\boldsymbol{\sigma}_p$, $\boldsymbol{\varepsilon}_p$ on planes orthogonal to Ω:

$$\boldsymbol{\sigma}_p^T = \left\{ \begin{array}{ccc} \sigma_{yy} & \sigma_{zz} & \sigma_{yz} \end{array} \right\} \quad \boldsymbol{\varepsilon}_p^T = \left\{ \begin{array}{ccc} \varepsilon_{yy} & \varepsilon_{zz} & \varepsilon_{yz} \end{array} \right\} \tag{3}$$

Under the hypothesis of linear analysis, the following strain-displacement geometrical relations hold:

$$\begin{aligned} \boldsymbol{\varepsilon}_n^T &= \left\{ \begin{array}{ccc} u_{x,x} & u_{x,y} + u_{y,x} & u_{x,z} + u_{z,x} \end{array} \right\} \\ \boldsymbol{\varepsilon}_p^T &= \left\{ \begin{array}{ccc} u_{y,y} & u_{z,z} & u_{y,z} + u_{z,y} \end{array} \right\} \end{aligned} \tag{4}$$

Subscripts 'x', 'y' and 'z', when preceded by comma, stand for derivation versus the corresponding spatial coordinate. A compact vectorial notation can be adopted for Eqs. (4):

$$\begin{aligned} \boldsymbol{\varepsilon}_n &= \mathbf{D}_{np}\mathbf{u} + \mathbf{D}_{nx}\mathbf{u} \\ \boldsymbol{\varepsilon}_p &= \mathbf{D}_p\mathbf{u} \end{aligned} \tag{5}$$

where $\mathbf{D}_{np}$, $\mathbf{D}_{nx}$ and $\mathbf{D}_p$ are the following differential matrix operators:

$$\mathbf{D}_{np} = \begin{bmatrix} 0 & 0 & 0 \\ \dfrac{\partial}{\partial y} & 0 & 0 \\ \dfrac{\partial}{\partial z} & 0 & 0 \end{bmatrix} \quad \mathbf{D}_{nx} = \mathbf{I}\dfrac{\partial}{\partial x} \quad \mathbf{D}_p = \begin{bmatrix} 0 & \dfrac{\partial}{\partial y} & 0 \\ 0 & 0 & \dfrac{\partial}{\partial z} \\ 0 & \dfrac{\partial}{\partial z} & \dfrac{\partial}{\partial y} \end{bmatrix} \tag{6}$$

and $\mathbf{I}$ is the unit matrix.

The constitutive equations are:

$$\begin{aligned} \boldsymbol{\sigma}_p &= \mathbf{C}_{pp}\boldsymbol{\varepsilon}_p + \mathbf{C}_{pn}\boldsymbol{\varepsilon}_n \\ \boldsymbol{\sigma}_n &= \mathbf{C}_{np}\boldsymbol{\varepsilon}_p + \mathbf{C}_{nn}\boldsymbol{\varepsilon}_n \end{aligned} \tag{7}$$

The matrices $\mathbf{C}_{pp}$, $\mathbf{C}_{pn}$, $\mathbf{C}_{np}$ and $\mathbf{C}_{nn}$ in Eqs. (7) are:

$$\mathbf{C}_{pp} = \begin{bmatrix} C_{22} & C_{23} & 0 \\ C_{23} & C_{33} & 0 \\ 0 & 0 & C_{44} \end{bmatrix} \quad \mathbf{C}_{pn} = \mathbf{C}_{np}^T = \begin{bmatrix} C_{12} & 0 & 0 \\ C_{13} & 0 & 0 \\ 0 & 0 & 0 \end{bmatrix} \quad \mathbf{C}_{nn} = \begin{bmatrix} C_{11} & 0 & 0 \\ 0 & C_{66} & 0 \\ 0 & 0 & C_{55} \end{bmatrix} \tag{8}$$

Coefficients C_{ij} as function of the Young's modulus and Poisson ratios are not here presented for the sake of brevity. They can be found in Reddy [44].

3 Displacement Field Approximation

The displacement field is a priori assumed over the cross-section in the following manner:

$$\mathbf{u}\left(x, y, z\right) = F_\tau\left(y, z\right)\mathbf{u}_\tau\left(x\right) \quad \text{with} \quad \tau = 1,\ 2,\ \ldots,\ N_u \tag{9}$$

According to Einstein's notation, subscript τ implicitly represents a summation. $F_\tau\left(y, z\right)$ is a generic expansion function over the cross-section and N_u is the number of accounted terms.

This kinematic formulation allows to account for several beam theories since the choice of the expansion functions $F_\tau\left(y, z\right)$ and order N_u is arbitrary. In this study, Mac Laurin's polynomials are used as approximating

functions F_τ. N_u and F_τ as functions of the order of the theory N are obtained through Pascal's triangle as shown in Table 1.

The explicit form of a generic N-order displacement field reads:

$$
\begin{aligned}
u_x &= u_{x1} + u_{x2}y + u_{x3}z + \cdots + u_{x\frac{(N^2+N+2)}{2}}y^N + \cdots + u_{x\frac{(N+1)(N+2)}{2}}z^N \\
u_y &= u_{y1} + u_{y2}y + u_{y3}z + \cdots + u_{y\frac{(N^2+N+2)}{2}}y^N + \cdots + u_{y\frac{(N+1)(N+2)}{2}}z^N \\
u_z &= u_{z1} + u_{z2}y + u_{z3}z + \cdots + u_{z\frac{(N^2+N+2)}{2}}y^N + \cdots + u_{z\frac{(N+1)(N+2)}{2}}z^N
\end{aligned}
\tag{10}
$$

As far as the displacements variation along the beam axis is concerned, a one-dimensional finite element approximation is used:

$$
\mathbf{u}(x,y,z) = F_\tau(y,z)\,N_i(x)\,\mathbf{q}_{\tau i} \quad \text{with} \quad \tau = 1,\ 2,\ \ldots,\ N_u \quad \text{and} \quad i = 1,\ 2,\ \ldots,\ N_n^e
\tag{11}
$$

$N_i(x)$ is a C^0 shape function, N_n^e the number of nodes per element and $\mathbf{q}_{\tau i}$ the nodal displacement unknown vector. Linear, quadratic and cubic elements based on Lagrangian shape functions are considered. They are referred to as "B2", "B3" and "B4", respectively. The corresponding shape functions are not presented. They can be found in Bathe [45].

Timoshenko's beam theory:

$$
\begin{aligned}
u_x &= u_{x1} + u_{x2}y + u_{x3}z \\
u_y &= u_{y1} \\
u_z &= u_{z1}
\end{aligned}
\tag{12}
$$

is derived from the first-order approximation model. In TBT, no shear correction coefficient is considered, since it depends upon several parameters, such as geometry of the cross-section (see, for instance, Cowper [46] and Murty [47]). Higher-order models yield a more detailed description of the shear mechanics (no shear correction coefficient is required), of the in- and out-of-section deformations, of the coupling of the spatial directions due to Poisson's effect and of the torsional mechanics than classical models do. TBT model accounts for constant shear stress and strain components. Regarding classical models, the material stiffness coefficients should be corrected in order to contrast a phenomenon known in literature as Poisson's locking (see Giunta et al. [40]). A reduced material stiffness coefficient is obtained by imposing σ_{yy} and σ_{zz} equals to zero in Hooke's law. Consequently, an algebraic linear system in ε_{yy} and ε_{zz} is obtained. By substituting its solution into σ_{xx} Hooke's equation, the reduced stiffness coefficient Q_{11} is obtained:

$$
Q_{11} = C_{11} + C_{12}\frac{C_{12}C_{33} - C_{13}C_{23}}{C_{23}^2 - C_{22}C_{33}} + C_{13}\frac{C_{22}C_{13} - C_{12}C_{23}}{C_{23}^2 - C_{22}C_{33}}
\tag{13}
$$

4 Principle of Virtual Displacements

The stiffness and the mass matrices are obtained via the Principle of Virtual Displacements, see Reddy [48]:

$$
\delta L_i + \delta L_\rho = 0
\tag{14}
$$

δ symbolises a virtual variation, L_i stands for the strain energy and L_ρ for the inertial work.

4.1 Virtual variation of the strain energy

Coherently with the grouping of the stress and strain components in Eqs. (2) and (3), the virtual variation of the strain energy can be considered as the sum of two contributes:

$$
\delta L_i = \int\limits_{le}\int\limits_{\Omega} \left(\delta\boldsymbol{\epsilon}_n^T \boldsymbol{\sigma}_n + \delta\boldsymbol{\epsilon}_p^T \boldsymbol{\sigma}_p \right) d\Omega dx
\tag{15}
$$

where l_e is the length of an element. By replacing the geometrical relations, Eqs. (5), the material constitutive equations, Eqs. (7), and the unified hierarchical approximation of the displacements in Eq. (9), Eq. (15) becomes:

$$
\begin{aligned}
\delta L_{\mathrm{i}} = \quad & \delta \mathbf{q}_{\tau i}^T \int\limits_{l_e} \int\limits_{\Omega} \left\{ (\mathbf{D}_{nx} N_i)^T F_\tau \left[\mathbf{C}_{np} (\mathbf{D}_p F_s) N_j + \mathbf{C}_{nn} (\mathbf{D}_{np} F_s) N_j + \mathbf{C}_{nn} F_s (\mathbf{D}_{nx} N_j) \right] \right. \\
& + (\mathbf{D}_{np} F_\tau)^T N_i \left[\mathbf{C}_{np} (\mathbf{D}_p F_s) N_j + \mathbf{C}_{nn} (\mathbf{D}_{np} F_s) N_j + \mathbf{C}_{nn} F_s (\mathbf{D}_{nx} N_j) \right] \\
& \left. + (\mathbf{D}_p F_\tau)^T N_i \left[\mathbf{C}_{pp} (\mathbf{D}_p F_s) N_j + \mathbf{C}_{pn} (\mathbf{D}_{np} F_s) N_j + \mathbf{C}_{pn} F_s (\mathbf{D}_{nx} N_j) \right] \right\} d\Omega \ dx \ \mathbf{q}_{sj}
\end{aligned}
$$

This latter can be written in the following compact vector form:

$$
\delta L_{\mathrm{i}} = \delta \mathbf{q}_{\tau i}^T \mathbf{K}^{\tau s i j} \mathbf{q}_{sj}. \tag{16}
$$

The components of the stiffness matrix fundamental nucleus $\mathbf{K}^{\tau s i j} \in \mathbb{R}^{3 \times 3}$ are:

$$
\begin{aligned}
K_{xx}^{\tau s i j} &= I_{i,x j,x} J_{\tau s}^{11} + I_{i,x j} J_{\tau s,y}^{16} + I_{i j,x} J_{\tau,y s}^{16} + I_{ij} \left(J_{\tau,z s,z}^{55} + J_{\tau,y s,y}^{66} \right) \\
K_{xy}^{\tau s i j} &= I_{i j,x} J_{\tau,y s}^{12} + I_{i,x j,x} J_{\tau s}^{16} + I_{ij} \left(J_{\tau,y s,y}^{26} + J_{\tau,z s,z}^{45} \right) + I_{i,x j} J_{\tau s,y}^{66} \\
K_{xz}^{\tau s i j} &= I_{i j,x} J_{\tau,z s}^{13} + I_{ij} \left(J_{\tau,z s,y}^{36} + J_{\tau,y s,z}^{45} \right) + I_{i,x j} J_{\tau s,z}^{55} \\
K_{yx}^{\tau s i j} &= I_{i,x j} J_{\tau s,y}^{12} + I_{i,x j,x} J_{\tau s}^{16} + I_{ij} \left(J_{\tau,y s,y}^{26} + J_{\tau,z s,z}^{45} \right) + I_{i j,x} J_{\tau,y s}^{66} \\
K_{yy}^{\tau s i j} &= I_{ij} \left(J_{\tau,y s,y}^{22} + J_{\tau,z s,z}^{44} \right) + I_{i j,x} J_{\tau,y s}^{26} + I_{i,x j} J_{\tau s,y}^{26} + I_{i,x j,x} J_{\tau s}^{66} \\
K_{yz}^{\tau s i j} &= I_{ij} \left(J_{\tau,z s,y}^{23} + J_{\tau,y s,z}^{44} \right) + I_{i j,x} J_{\tau,z s}^{36} + I_{i,x j} J_{\tau s,z}^{45} \\
K_{zx}^{\tau s i j} &= I_{i,x j} J_{\tau s,z}^{13} + I_{ij} \left(J_{\tau,y s,z}^{36} + J_{\tau,z s,y}^{45} \right) + I_{i j,x} J_{\tau,z s}^{55} \\
K_{zy}^{\tau s i j} &= I_{ij} \left(J_{\tau,y s,z}^{23} + J_{\tau,z s,y}^{44} \right) + I_{i,x j} J_{\tau s,z}^{36} + I_{i j,x} J_{\tau,z s}^{45} \\
K_{zz}^{\tau s i j} &= I_{ij} \left(J_{\tau,z s,z}^{33} + J_{\tau,y s,y}^{44} \right) + I_{i j,x} J_{\tau,y s}^{45} + I_{i,x j} J_{\tau s,y}^{45} + I_{i,x j,x} J_{\tau s}^{55}
\end{aligned} \tag{17}
$$

The generic term $J_{\tau_{(,\phi)} s_{(,\xi)}}^{gh}$ is a cross-section moment and it stands for:

$$
J_{\tau_{(,\phi)} s_{(,\xi)}}^{gh} = \int\limits_{\Omega} C_{gh} F_{\tau_{(,\phi)}} F_{s_{(,\xi)}} \ d\Omega \tag{18}
$$

It is a weighted sum (in the continuum) of each elemental cross-section area where the weight functions account for the spatial distribution of the geometry and material. $I_{i_{(,x)} j_{(,x)}}$ is an integral over the axial coordinate of the shape functions or their derivatives:

$$
I_{i_{(,x)} j_{(,x)}} = \int\limits_{l_e} N_{i_{(,x)}} N_{j_{(,x)}} \ dx \tag{19}
$$

These integrals are evaluated numerically through Gauss' quadrature method. In order to correct the shear locking, a selective integration technique is used. Two, three and four quadrature points are used for the full integration for B2, B3 and B4 elements, respectively. One point less is used for the under-integrated term I_{ij} in $K_{xx}^{\tau s i j}$ that is related to shear deformations γ_{xy} and γ_{xz}.

4.2 Virtual variation of the inertial work

The virtual variation of the inertial work is:

$$
\delta L_\rho = \int\limits_{l} \int\limits_{\Omega} \rho \delta \mathbf{u} \ddot{\mathbf{u}} \ d\Omega \ dx \tag{20}
$$

where ρ is the material density and double dots stand for second derivative versus time. Accounting for Eq. (9), Eq. (20) becomes:

$$\delta L_\rho = \delta \mathbf{q}_{\tau i}^T \int_{le} N_i N_j dx \int_\Omega \rho F_\tau F_s d\Omega \; \ddot{\mathbf{q}}_{sj} \tag{21}$$

and its compact vectorial form is:

$$\delta L_\rho = \delta \mathbf{q}_{\tau i}^T \; \mathbf{M}^{\tau s} \; \ddot{\mathbf{q}}_{sj} \tag{22}$$

The components of the inertial matrix $\mathbf{M}^{\tau s}$ are:

$$\mathbf{M}_{lm}^{\tau sij} = \delta_{lm} I_{ij} J_{\tau s}^\rho \quad \text{with } l, m = x, y, z \tag{23}$$

in which δ_{lm} is Kronecker's delta and $J_{\tau s}$ is the following integral:

$$J_{\tau s}^\rho = \int_\Omega \rho F_\tau F_s \; d\Omega \tag{24}$$

4.3   Eigenvalue Problem

The final eigenvalue problem is rewritten in terms of the global stiffness (K) and mass (M) matrices:

$$\mathbf{M}\ddot{\mathbf{q}} + \mathbf{K}\mathbf{q} = 0 \tag{25}$$

where, $\mathbf{q}$ is the global vector for the nodal unknowns:

$$\mathbf{q} = \overline{\mathbf{q}} e^{i\omega t} \tag{26}$$

t stands for the time, ω represents the angular frequency, $\overline{\mathbf{q}}$ is the global unknown vector and i is the imaginary unit. The final eigenvalue problem, then, reads:

$$(\mathbf{K} - \omega^2 \mathbf{M})\overline{\mathbf{q}} = 0 \tag{27}$$

5   Numerical Results and Discussion

The free vibration of sandwich beams, as shown in Fig. 2, under simply supported, cantilever, and clamped-clamped boundary conditions are studied. The cross section sides a and b are both equal to 0.02 m (the cross-section is square) and the face sheets thickness h_f is 0.003 m. A length-to-thickness ratio l/a as high as 100 (slender beams) and as low as 10 (short beams) is considered. Material properties for the face sheets are: $E_f = 200$ GPa, $\nu_f = 0.30$ and $\rho_f = 7800$ kg/m^3. For the core, they are: $E_c = 0.66$ GPa, $\nu_c = 0.27$ and $\rho_c = 60$ kg/m^3.

Results are compared with three-dimensional finite element solutions obtained via the commercial code Ansys. The quadratic solid element 'SOLID 186' is used. In order to verify the convergence of the reference solution, an accuracy up to four significant digit for all the considered results is sought, different meshes are considered for both slender and short beams. For slender beams, the refined mesh is $70 \times 40 \times (5, 30)$, whereas the coarse one is $50 \times 10 \times (2, 6)$. As far as short beams are concerned, the refined mesh is $40 \times 40 \times (5, 30)$, whereas the coarse one is $10 \times 10 \times (2, 6)$. The first two numbers represent the number of elements along the beam axis (Ne_x) and width (Ne_y), respectively, whereas the numbers between brackets stand for elements number along the thickness of the face sheets and the core. Ne_z is the total number of elements along the

8

thickness. The same number of elements along the height and width is used ($Ne_z = Ne_y = n$). The generic three-dimensional FEM solution is named as 'FEM 3D$_n$'.

As far as the computational cost are concerned, the degrees of freedom (DOF) for the three-dimensional finite element model using 'SOLID 186' as a function of Ne_x and n are:

$$DOF_{3D} = 3\left[2Ne_x\left(2n^2 + 3n + 1\right) + 3n^2 + 4n + 1\right] \qquad (28)$$

For a fixed approximation order N, the total DOFs of the proposed solutions are:

$$DOF_{UF} = \frac{3(N+1)(N+2)}{2}N_n \qquad (29)$$

N_n stands for the total nodes number along the beam axis for the proposed elements. Some considerations about computational cost can be addressed here based on the two equations above. For the highest considered expansion order ($N = 19$), the degrees of freedom for a cross-section are 630 and DOF_{UF} is 321′930 for slender beams (511 nodes along the beam axis) and 189′630 for short beams (301 nodes). For slender beams, DOF_{3D} is 1′409′703 for $70 \times 40 \times (5, 30)$. For short beams, DOF_{3D} is 811′923 for $40 \times 40 \times (5, 30)$.

The natural frequencies are put into the following dimensionless form:

$$\overline{\omega} = \frac{l^2}{a}\sqrt{\frac{\rho_f}{E_f}}\,\omega \qquad (30)$$

Mode comparison has been done by visualisation within the Ansys post-processing environment. The proposed solution has been exported to Ansys by imposing at each node the displacement components computed by the proposed models trough Ansys parametric design language command `DNSOL`. For the sake of brevity, no figure comparing the modal shapes have been presented. They can be found in Giunta et al. [41].

5.1 Simply supported beams

Simply supported beams are first investigated. In order to present a convergence analysis versus the total node number, results provided by the finite elements method are assessed towards an exact Navier-type analytical solution (see Giunta et al. [41]). The first vibration mode for a short beam (bending on plane xz) is considered. This boundary condition type is obtained by posing equal to zero u_y and u_z at $x/l = 0$ and 1 and u_x at $x/l = 0.5$. The latter condition is used to remove the rigid body motion along the beam axis and since the first three mode with a half wave number equal to one are considered It also allows to obtain a positive definite stiffness matrix that can be factorised by means of Cholesky's method in the solution of the generalised eigenvalue problem. It should be noticed that for the most general case (valid for any number of half waves along the axis), the condition $u_x 0$ at $x/l = 0.5$ should be removed. The natural frequencies relative error versus the dimensionless distance between two consecutive nodes δ_{ii+1}/l is evaluated for linear elements as presented in Fig. 3. δ_{ii+1}/l varies from 0.5 (number of nodes equals to 3) to $0.0000019\overline{2}$ ($N_n = 1′903$). Results have been obtained by $N = 5$. Solutions for different expansion orders N, length-to-width ratio values and number of nodes per element are very similar and they are not presented for the sake of brevity. The results that follow have been obtained using 301 and 511 nodes for short and slender beams, respectively. In order to avoid the shear-locking phenomenon, a selective integration technique was adopted. Fig. 4 shows the comparison between selective and full integration strategies. The variation of the ratio $\omega^{FEM}/\omega^{NAV}$ computed for the bending mode in the plane xy via B2 element versus l/a is presented. The selective

integration is free of locking and it is effective regardless the beam theory order N. The frequency computed by full integration is higher than the reference Navier solution since shear locking results in a higher bending stiffness. Similar results can be obtained for the bending mode in the plane xz. Both full and selective integration yield accurate frequencies for the torsional mode because torsional stiffness is not affected by the shear-locking.

Table 2 shows the first three frequencies with a half wave for slender beams. In all the tables, the frequencies are arranged according to the order of apparition in the Ansys model. The relative difference between the results provided by theories with order $N \geq 15$ and three-dimensional reference solution is about 4% (torsional mode), at worst. Results for short beams ($l/a = 10$) are presented in Table 3. It should be noted that the first two bending frequencies swapped the order of apparition when compared to slender beams. The first mode is bending with one half-wave in the plane xz, the second one corresponds to bending with one half-wave in the plane xy and the last one is torsion. The percentage error between the reference FEM $3D_{40}$ model and $N = 19$ model is 3.8% for the first mode and 2.1% for the third mode. The second mode is accurately predicted. The accuracy in predicting the frequency of flexural mode on plane xy is higher than that for flexural mode in the plane xz. This is due to the fact that in the latter bending mode occurs on a plane where material properties change discretely along the thickness direction (for a fixed value of the through-the-width coordinate) whereas in the former, for a fixed value of the through-the-thickness coordinate, they are constant, see Giunta et al. [41].

5.2   Cantilever beams

Frequencies and modes for slender cantilevered beams are presented in Tables 4 to 6. The first nine modes are considered. They are: bending in the plane xy with one, two, four, five, six half-waves, bending mode in the plane xz with one, two, four, five half-waves. A good agreement with the reference three-dimensional FEM solution can be observed for $N = 18$ where the highest relative difference is 2.8% (torsional mode). Except for flexural modes in the plane xy, TBT as well as low order models ($N \leq 5$) do not accurately predict the frequencies. The frequencies of short beams are presented in Tables 7 to 9. The first nine modes are: bending in the plane xy with one, two half-waves, bending in the plane xz with one, two, four, five, six half-waves and torsion. TBT cannot predict torsional modes due to the limit of theory hypothesis, but the results of bending modes related with xy are accurate. Higher-order theories match the reference three-dimensional finite element solution. The error for N equal to 17 is 4.7%, at worst, for the bending mode in plane xz with four half-waves. Several modes like bending mode in the plane xy (Mode 2 and 6) can be accurately predicted by higher-order models with $N \geq 7$ where the error is lower than 0.02%. Higher-order modes calls for a very rich displacement field. Refined models should be, therefore, used.

5.3   Clamped-clamped beams

The frequencies for $l/a = 100$ under clamped-clamped boundary condition are presented in Tables 10 to 12. The first nine modes are: bending with one, two, three and four half-waves in the plane xy, bending mode with one, two, three, four and five half-waves in the plane xz and torsion. The relative difference between results provided by a theory with N as low as 16 and the reference solution is lower than 3.1% (bending mode in the plane xz with four half-waves). It is interesting to note that the TBT model can accurately predict

the results related to flexural modes in the plane xy being the relative difference lower than 0.01%. Tables 13 to 15 present the dimensionless frequencies in the case of short beams. The modes for this case are: bending with in the plane xz with one, two, three, four, five and six half-waves, bending mode in the plane xy with one and two half-waves and two torsional modes. The relative difference between the results provided by theories with $N > 16$ and the three-dimensional reference solution is about 5.0% (bending in the plane xz with one half wave), at worst. As already observed, TBT and low-order theories ($N \leq 5$) are only able to accurately predict the bending mode in the plane xy. Higher-order models ($N \geq 6$) are required to predict the torsional frequencies.

6 Conclusions

Several higher-order one-dimensional beam finite elements have been presented. They have been derived through a Unified Formulation that allows to obtain the stiffness and mass matrices in a compact form. Timoshenko's beam model has been obtained as a special case. A free vibration analysis of sandwich beams has been addressed. Simply supported, cantilever and clamped-clamped sandwich beams have been investigated with different length-to-width ratio values. By comparing the results with three-dimensional finite elements solution obtained through the commercial code Ansys, it can be concluded that higher-order theory yield reasonably accurate results (being the maximal error as high as about 5% in the worst case) with a reduced computation cost (up to four times) compared to the reference solutions. Considering the difference in accuracy for some higher-order modes, further improvements in the models can be obtained by accounting for a layer-wise approach or by using a C^0 continuous over the cross-section ("zig-zag" function) within the equivalent single layer approach.

Acknowledgements

References

[1] H. G. Allen. Analysis and design of structural sandwich panels. *Pergamon Press.*, 1969.

[2] E. Carrera. Historical review of zig-zag theories for multilayered plates and shells. *Applied Mechanics Reviews*, 56(3):287–308, 2003.

[3] H. Hu, S. Belouettar, M. Potier-Ferry, E. M. Daya. Review and assessment of various theories for modeling sandwich composites. *Composites Structures*, 84(3):282–292, 2008.

[4] K. M. Ahmed. Free vibration of curved sandwich beams by the method of finite elements. *Journal of Sound and Vibration*, 18(1):61–74, 1971.

[5] S. K. Goyal, P. K. Sinha. A note on free vibration of sandwich beams with central mass. *Journal of Sound and Vibration*, 49(3):437–441, 1976.

[6] D. Shu. Vibration of sandwich beams with double delaminations. *Composites Science and Technology*, 54(1):101–109, 1995.

[7] Y. Frostig, M. Baruch. Free vibrations of sandwich beams with a transversely flexible core: a high order approach. *Journal of Sound and Vibration*, 176(2):195–208, 1994.

[8] T. Sakiyama, H. Matsuda, C. Morita. Free vibration analysis of sandwich beams with elastic or viscoelastic core by applying the discrete Green function. *Journal of Sound and Vibration*, 191(2):189–206, 1996.

[9] T. Sakiyama, H. Matsuda, C. Morita. Free vibration analysis of continuous sandwich beams with elastic or viscoelastic cores by applying the discrete Green function. *Journal of Sound and Vibration*, 198(4):439–454, 1996.

[10] M. Kameswara Rao, Y.M. Desai, M.R. Chitnis. Free vibrations of laminated beams using mixed theory. *Composite Structures*, 52(2):149–160, 2001.

[11] E. M. Daya, M. Potier-Ferry. A numerical method for nonlinear eigenvalue problems application to vibration of viscoelastic structures. *Computers and Structures*, 79(5):533–541, 2001.

[12] J. R. Banerjee. Free vibration of sandwich beams using the dynamic stiffness method. *Computers and Structures*, 81(18):1915–1922, 2003.

[13] J.R. Banerjee, C.W. Cheung, R. Morishima, M. Perera, J. Njuguna. Free vibration of a three-layered sandwich beam using the dynamic stiffness method and experiment. *International Journal of Solids and Structures*, 44(22):7543–7563, 2007.

[14] S. Kapuria, P.C. Dumir, N.K. Jain. Assessment of zigzag theory for static loading, buckling, free and forced response of composite and sandwich beams. *Composite Structures*, 64(3):317–327, 2004.

[15] R. K. Bhangale, N. Ganesan. Thermoelastic buckling and vibration behavior of a functionally graded sandwich beam with constrained viscoelasic core. *Journal of Sound and Vibration*, 295(1):294–316, 2006.

[16] Z. Wu, W. Chen. An assessment of several displacement-based theories for the vibration and stability analysis of laminated composite and sandwich beams *Composite Structures*, 84(4):337–349, 2008.

[17] M. Chehel Amirani, S.M.R. Khalili, N. Nemati. Free vibration analysis of sandwich beam with FG core using the element free Galerkin method. *Composite Structures*, 90(3):373–379, 2009.

[18] H. Arvin, M. Sadighi, A.R. Ohadi A numerical study of free and forced vibration of composite sandwich beam with viscoelastic core. *Composite Structures*, 92(4):996–1008, 2010.

[19] P. Vidal, O. Polit Vibration of multilayered beams using sinus finite elements with transverse normal stress. *Composite Structures*, 92(4):1524–1534, 2010.

[20] A.R. Damanpack, S.M.R. Khalili. High-order free vibration analysis of sandwich beams with a flexible core using dynamic stiffness method. *Composite Structures*, 94(5):1503–1514, 2012.

[21] J. Lou, B. Wang, L. Ma, L. Wu. Free vibration analysis of lattice sandwich beams under several typical boundary conditions. *Acta Mechanica Solida Sinica*, 26(5):458–467, 2013.

[22] M. Xu, Z. Qiu. Free vibration analysis and optimization of composite lattice truss core sandwich beams with interval parameters. *Composite Structures*, 106:85–95, 2013.

[23] Y. Yang, C.C. Lam, K.P. Kou, V.P. Lu. Free vibration analysis of the functionally graded sandwich beams by a meshfree boundary-domain integral equation method. *Composite Structures*, 117:32–39, 2014.

[24] Y. Qu, S. Wu, H. Li, G. Meng. Three-dimensional free and transit vibration analysis of composite laminated and sandwich rectangular parallelepipeds: Beams, plates and solids. *Composites: Part B*, 73:96–110, 2015.

[25] G. He, D. Wang, X. Yang. Analytical solution for free vibration and buckling of composite beams using a higher order beam theory. *Acta Mechanica Sinica*, 29(3):300–315, 2016.

[26] G. Jin, C. Yang, Z. Liu. Vibration and damping analysis of sandwich viscoelastic-core beam using Reddy's higher-order theory. *Composite Structures*, 140:390–409, 2016.

[27] D. Chen, S. Kitipornchai, J. Yang. Nonlinear free vibration of shear deformable sandwich beam with a functionally graded porous core. *Thin-walled Structures*, 107:39–48, 2016.

[28] M. Pradhan, M. K. Mishra, P.R. Dash. Free vibration analysis of an asymmetric sandwich beam resting on a variable Pasternak foundation. *Procedia Engineering*, 144:116–123, 2016.

[29] E. Sadeghpour, M. Sadighi, Abdolreza Ohadi. Free vibration analysis of a debonded curved sandwich beams. *European Journal of Mechanics A/Solids*, 57:71–84, 2016.

[30] P. Tossapanon, N. Wattanasakulpong. Stability and free vibration of functionally graded sandwich beams resting on two-parameter elastic foundation. *Composite Structures*, 142:215–225, 2016.

[31] E. Carrera. Theories and finite elements for multilayered plates and shells: a unified compact formulation with numerical assessment and benchmarking. *Archives of Computational Methods in Engineering*, 10(3):216–296, 2003.

[32] E. Carrera and G. Giunta. Exact, hierarchical solutions for localised loadings in isotropic, laminated and sandwich shells. *Journal of Pressure Vessel Technology*, 131(4):0412021–04120214, 2009.

[33] G. Giunta, F. Biscani, S. Belouettar, and E. Carrera. Hierarchical modelling of doubly curved laminated composite shells under distributed and localised loadings. *Composites: Part B*, 42(4):682–691, 2011.

[34] E. Carrera, G. Giunta, P. Nali, and M. Petrolo. Refined beam elements with arbitrary cross-section geometries. *Computers and Structures*, 88(5-6):283–293, 2010.

[35] E. Carrera, G. Giunta, and M. Petrolo. *Beam Structures: Classical and Advanced Theories.* John Wiley and Sons, 2011.

[36] G. Giunta, S. Belouettar, and E. Carrera. Analysis of FGM beams by means of classical and advanced theories. *Mechanics of Advanced Materials and Structures*, 17(8):622–635, 2010.

[37] G. Giunta, F. Biscani, E. Carrera, and S. Belouettar. Analysis of thin-walled beams via a one-dimensional unified formulation. *International Journal of Applied Mechanics*, 3(3):407–434, 2011.

[38] G. Giunta, D. Crisafulli, S. Belouettar, and E. Carrera. Hierarchical theories for the free vibration analysis of functionally graded beams. *Composite Structures*, 94(1):68–74, 2011.

[39] Q. Z. He, H. Hu, S. Belouettar, G. Giunta, K. Yu, Y. Liu, F. Biscani, E. Carrera, M. Potier-Ferry. Multi-scale modelling of sandwich structures using hierarchical kinematics. *Composite Structures*, 93(9):2375–2383, 2011.

[40] G. Giunta, F. Biscani, S. Belouettar, Ferreira A. J. M, and E. Carrera. Free vibration analysis of composite beams via refined theories. *Composites: Part B*, 44(1): 540–552, 2013.

[41] G. Giunta, M. Metla, Y.Koutsawa, S.Belouettar. Free vibration and stability analysis of three-dimensional sandwich beams via hierarchical models. *Composites: Part B*, 47:326–338, 2013.

[42] G. Giunta, Y. Koutsawa, S. Belouettar, H. Hu. Static, free vibration and stability analysis of three-dimensional nano-beams by atomistic refined models accounting for surface free energy effect. *International Journal of Solids and Structures*, 50(9):1460–1472, 2013.

[43] R. E. D. Bishop, S. M. Cannon, and S. Miao. On coupled bending and torsional vibration of uniform beams. *Journal of Sound and Vibration*, 131(9):457–464, 1989.

[44] J. N. Reddy. *Mechanics of laminated composite plates and shells. Theory and Analysis.* CRC Press, 2nd edition, 2004.

[45] K. J. Bathe. *Finite Element Procedure.* Prentice Hall, 1996.

[46] G. R. Cowper. The shear co-efficient in Timoshenko beam theory. *Journal of Applied Mechanics*, 33(10):335–340, 1966.

[47] A. V. K. Murty. Analysis of short beams. *AIAA Journal*, 8(11):2098–2100, 1970.

[48] J. N. Reddy. *Energy Principles and Variational Methods in Applied Mechanics.* John Wiley and Sons, 2nd edition, 2002.

Figures
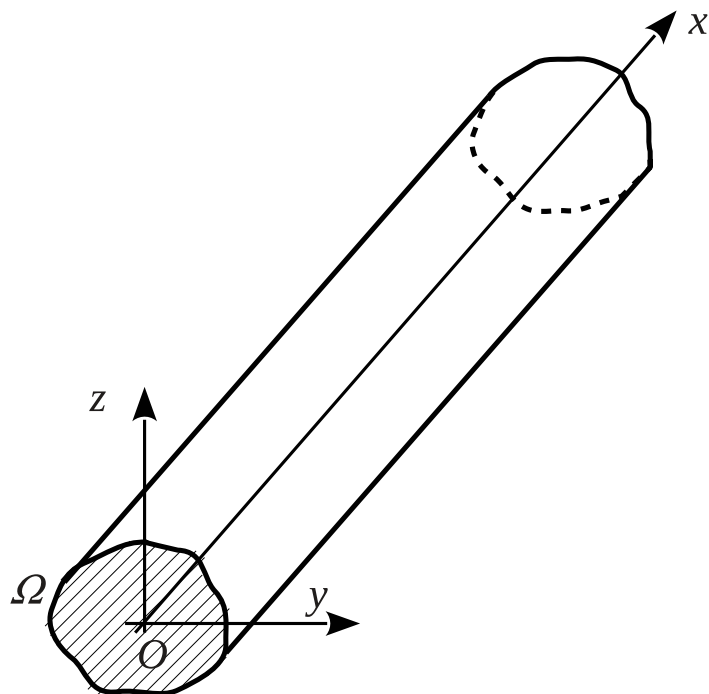
Figure 1: Beam structure and reference system.
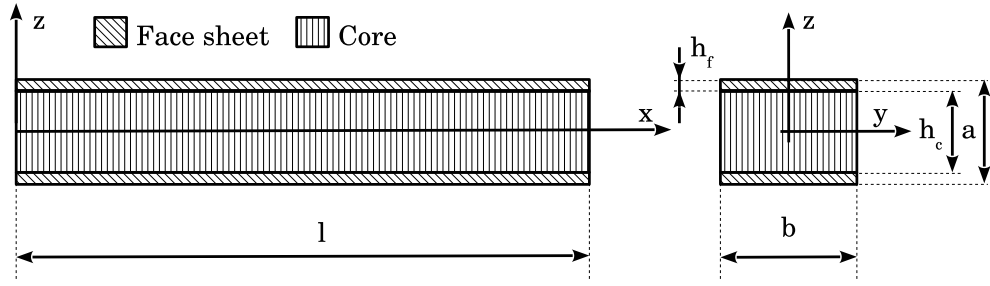
Figure 2: Sandwich beam geometry.
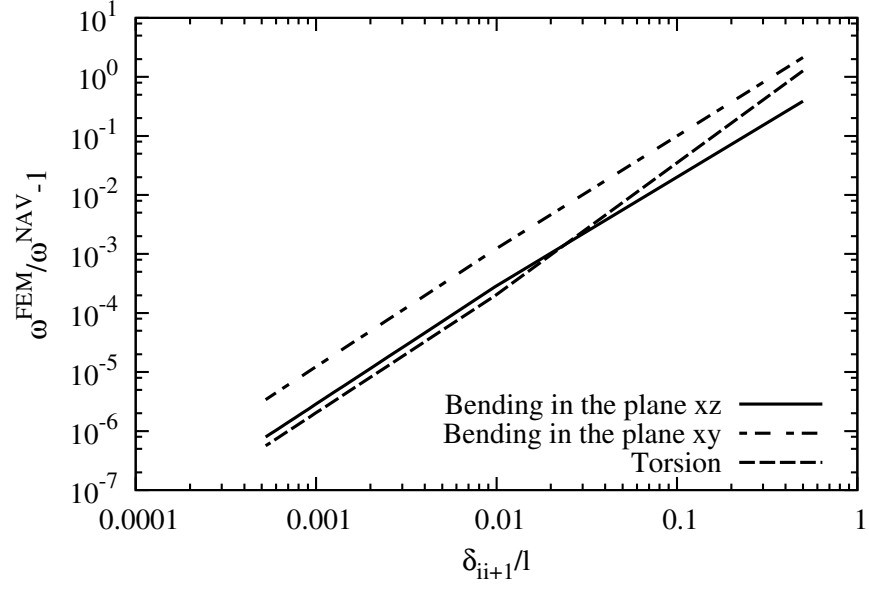
Figure 3: Relative natural frequencies error (with reference to Navier-closed form solution) versus the dimensionless distance between two consecutive nodes, simply supported short sandwich beam, linear elements and $N = 5$.
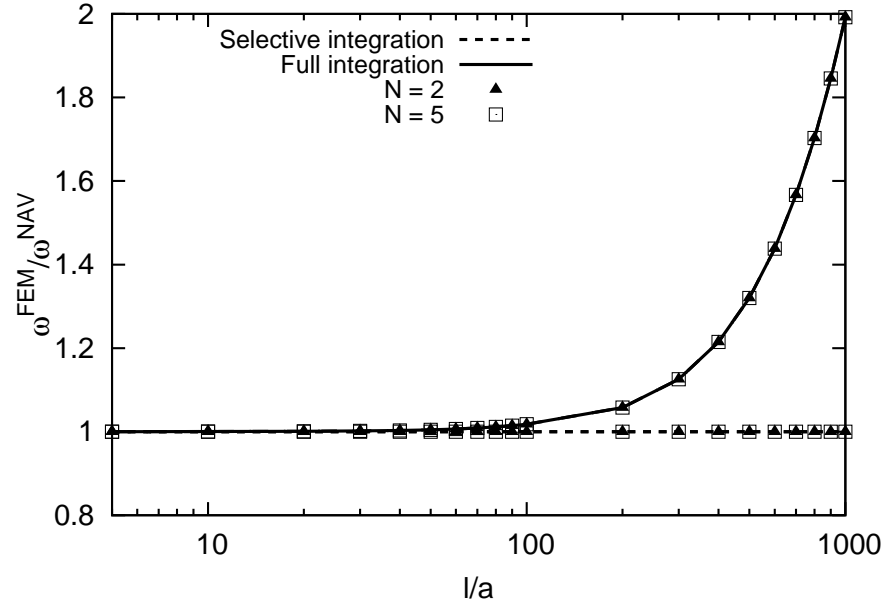
Figure 4: Shear locking correction via selective integration for B2 element, simply supported sandwich beams. Bending mode in the plane xy.

Tables

N	N_u	F_τ			
0	1	$F_1 = 1$			
1	3	$F_2 = y \quad F_3 = z$			
2	6	$F_4 = y^2 \quad F_5 = yz \quad F_6 = z^2$			
3	10	$F_7 = y^3 \quad F_8 = y^2z \quad F_9 = yz^2 \quad F_{10} = z^3$			
...	...	...			
N	$\frac{(N+1)(N+2)}{2}$	$F_{\frac{(N^2+N+2)}{2}} = y^N \quad F_{\frac{(N^2+N+4)}{2}} = y^{N-1}z \quad \ldots \quad F_{\frac{N(N+3)}{2}} = yz^{N-1} \quad F_{\frac{(N+1)(N+2)}{2}} = z^N$			

Table 1: Mac Laurin's polynomials terms via Pascal's triangle.

	Mode 1[1]			Mode 2[2]			Mode 3[3]		
	$\overline{\omega}$			$\overline{\omega}$			$\overline{\omega} \times 10^{-1}$		
FEM 3D$_{30}$	2.8344			4.1027			3.8975		
FEM 3D$_{10}$	2.8344			4.1027			3.8981		
	B2	B3	B4	B2	B3	B4	B2	B3	B4
$N = 18$	2.8345	2.8345	2.8345	4.1119	4.1119	4.1119	4.0064	4.0064	4.0064
$N = 17$	2.8345	2.8345	2.8345	4.1119	4.1119	4.1119	4.0070	4.0070	4.0070
$N = 16$	2.8345	2.8345	2.8345	4.1119	4.1119	4.1119	4.0070	4.0070	4.0070
$N = 15$	2.8345	2.8345	2.8345	4.1119	4.1119	4.1119	4.0529	4.0529	4.0529
$N = 14$	2.8345	2.8345	2.8345	4.1151	4.1151	4.1151	4.0530	4.0530	4.0530
$N = 13$	2.8345	2.8345	2.8345	4.1151	4.1151	4.1151	4.0555	4.0555	4.0555
$N = 12$	2.8345	2.8345	2.8345	4.1152	4.1152	4.1152	4.0555	4.0555	4.0555
$N = 11$	2.8345	2.8345	2.8345	4.1152	4.1152	4.1152	4.1523	4.1523	4.1523
$N = 10$	2.8345	2.8345	2.8345	4.1209	4.1209	4.1209	4.1523	4.1523	4.1523
$N = 9$	2.8345	2.8345	2.8345	4.1209	4.1209	4.1209	4.2153	4.2153	4.2153
$N = 8$	2.8345	2.8345	2.8345	4.1236	4.1236	4.1236	4.2153	4.2153	4.2153
$N = 7$	2.8345	2.8345	2.8345	4.1236	4.1236	4.1236	4.4285	4.4285	4.4285
$N = 6$	2.8345	2.8345	2.8345	4.1324	4.1324	4.1324	4.4286	4.4286	4.4286
$N = 5$	2.8346	2.8345	2.8345	4.1324	4.1324	4.1324	5.7207	5.7193	5.7294
$N = 4$	2.8346	2.8345	2.8345	4.1726	4.1726	4.1726	5.7208	5.7194	5.7295
$N = 3$	2.8346	2.8345	2.8345	4.1726	4.1726	4.1726	5.7229	5.7216	5.7321
$N = 2$	2.8346	2.8346	2.8346	4.1815	4.1815	4.1815	5.7277	5.7264	5.7363
TBT	2.8346	2.8345	2.7944	4.1815	4.1814	4.0562	$-$[4]	$-$	$-$

1: Bending mode in the plane xy with one half wave.

2: Bending mode in the plane xz with one half wave.

3: Torsional mode.

4: Mode not provided by the theory.

Table 2: Dimensionless natural frequencies of slender simply supported beams ($l/a = 100$), modes 1 to 3.

	Mode 1[1]	Mode 2[2]		Mode 3[3]		
	$\overline{\omega}$	$\overline{\omega}$		$\overline{\omega}$		
FEM 3D$_{40}$	1.9146	2.7897		4.4808		
FEM 3D$_{10}$	1.9146	2.7898		4.4814		
	B2,B3,B4	B2	B3, B4	B2	B3	B4
$N = 19$	1.9878	2.7901	2.7900	4.5750	4.5750	4.5750
$N = 18$	2.0060	2.7901	2.7900	4.5756	4.5756	4.5756
$N = 17$	2.0061	2.7901	2.7900	4.5762	4.5761	4.5761
$N = 16$	2.0064	2.7901	2.7900	4.5763	4.5763	4.5763
$N = 15$	2.0065	2.7901	2.7901	4.6150	4.6150	4.6150
$N = 14$	2.0414	2.7901	2.7901	4.6160	4.6160	4.6160
$N = 13$	2.0414	2.7901	2.7901	4.6182	4.6182	4.6182
$N = 12$	2.0429	2.7901	2.7901	4.6184	4.6184	4.6184
$N = 11$	2.0431	2.7901	2.7901	4.7003	4.7003	4.7003
$N = 10$	2.1117	2.7901	2.7901	4.7026	4.7026	4.7026
$N = 9$	2.1118	2.7901	2.7901	4.7563	4.7562	4.7562
$N = 8$	2.1465	2.7901	2.7901	4.7581	4.7581	4.7581
$N = 7$	2.1471	2.7901	2.7901	4.9403	4.9403	4.9403
$N = 6$	2.2754	2.7901	2.7901	4.9444	4.9443	4.9443
$N = 5$	2.2766	2.7901	2.7901	6.0712	6.0811	6.0824
$N = 4$	2.7901	3.4360	3.4360	7.4988	7.4987	7.4987
$N = 3$	2.7902	3.4368	3.4367	11.142	11.164	11.166
$N = 2$	2.7954	4.0568	4.0567	15.889	15.921	15.924
TBT	2.7944	4.0562	4.0562	$-$[4]	$-$	$-$

1: Bending mode in the plane xz with one half wave.

2: Bending mode in the plane xy with one half wave.

3: Torsional mode.

4: Mode not provided by the theory.

Table 3: Dimensionless natural frequencies of short simply supported beams ($l/a = 10$), modes 1 to 3.

	Mode 1[1]			Mode 2[2]			Mode 3[3]		
	$\overline{\omega}$			$\overline{\omega}$			$\overline{\omega}$		
FEM 3D$_{30}$	1.0100			1.4770			6.3267		
FEM 3D$_{10}$	1.0101			1.4771			6.3269		
	B2	B3	B4	B2	B3	B4	B2	B3	B4
$N = 18$	1.0102	1.0102	1.0101	1.4788	1.4787	1.4787	6.3281	6.3277	6.3274
$N = 17$	1.0102	1.0102	1.0101	1.4788	1.4787	1.4787	6.3281	6.3277	6.3274
$N = 16$	1.0102	1.0102	1.0101	1.4788	1.4787	1.4787	6.3281	6.3277	6.3274
$N = 15$	1.0102	1.0102	1.0101	1.4788	1.4787	1.4787	6.3282	6.3277	6.3274
$N = 14$	1.0102	1.0102	1.0101	1.4794	1.4793	1.4792	6.3282	6.3277	6.3274
$N = 13$	1.0102	1.0102	1.0101	1.4794	1.4793	1.4792	6.3282	6.3277	6.3274
$N = 12$	1.0102	1.0102	1.0101	1.4794	1.4793	1.4792	6.3282	6.3277	6.3274
$N = 11$	1.0102	1.0102	1.0101	1.4794	1.4793	1.4792	6.3282	6.3277	6.3274
$N = 10$	1.0102	1.0102	1.0101	1.4804	1.4803	1.4802	6.3282	6.3277	6.3274
$N = 9$	1.0102	1.0102	1.0101	1.4804	1.4803	1.4802	6.3282	6.3277	6.3274
$N = 8$	1.0102	1.0102	1.0101	1.4808	1.4807	1.4807	6.3282	6.3277	6.3274
$N = 7$	1.0102	1.0102	1.0101	1.4808	1.4807	1.4807	6.3282	6.3277	6.3275
$N = 6$	1.0103	1.0102	1.0101	1.4823	1.4822	1.4822	6.3282	6.3278	6.3275
$N = 5$	1.0103	1.0102	1.0102	1.4823	1.4822	1.4822	6.3285	6.3281	6.3278
$N = 4$	1.0103	1.0102	1.0102	1.4891	1.4890	1.4890	6.3286	6.3281	6.3278
$N = 3$	1.0105	1.0104	1.0104	1.4892	1.4891	1.4890	6.3298	6.3293	6.3292
$N = 2$	1.0107	1.0106	1.0106	1.4907	1.4906	1.4905	6.3311	6.3307	6.3306
TBT	1.0098	1.0098	1.0098	1.4898	1.4898	1.4898	6.3259	6.3259	6.3259

1: Bending mode in the plane xy with one half wave.

2: Bending mode in the plane xz with one half wave.

3: Bending mode in the plane xy with two half waves.

Table 4: Dimensionless natural frequencies of slender cantilever beams ($l/a = 100$), modes 1 to 3.

| | Mode 4[1] | | | Mode 5[2] | | | Mode 6[3] | | |
	$\overline{\omega}$			$\overline{\omega} \times 10^{-1}$			$\overline{\omega} \times 10^{-1}$		
FEM 3D$_{30}$	8.7981			1.7702			1.9817		
FEM 3D$_{10}$	8.7987			1.7702			1.9820		
	B2	B3	B4	B2	B3	B4	B2	B3	B4
$N = 18$	8.8575	8.8569	8.8566	1.7706	1.7704	1.7704	2.0363	2.0363	2.0362
$N = 17$	8.8575	8.8569	8.8566	1.7706	1.7704	1.7704	2.0366	2.0366	2.0365
$N = 16$	8.8577	8.8571	8.8567	1.7706	1.7704	1.7704	2.0367	2.0366	2.0366
$N = 15$	8.8577	8.8571	8.8568	1.7706	1.7704	1.7704	2.0596	2.0595	2.0595
$N = 14$	8.8779	8.8773	8.8770	1.7706	1.7704	1.7704	2.0596	2.0595	2.0595
$N = 13$	8.8779	8.8773	8.8770	1.7706	1.7704	1.7704	2.0609	2.0608	2.0608
$N = 12$	8.8787	8.8781	8.8778	1.7706	1.7704	1.7704	2.0609	2.0608	2.0608
$N = 11$	8.8788	8.8782	8.8778	1.7706	1.7704	1.7704	2.1092	2.1091	2.1091
$N = 10$	8.9158	8.9152	8.9149	1.7706	1.7704	1.7704	2.1093	2.1092	2.1092
$N = 9$	8.9158	8.9152	8.9149	1.7706	1.7704	1.7704	2.1407	2.1406	2.1406
$N = 8$	8.9333	8.9327	8.9324	1.7706	1.7704	1.7704	2.1408	2.1407	2.1407
$N = 7$	8.9334	8.9328	8.9325	1.7706	1.7705	1.7704	2.2472	2.2471	2.2471
$N = 6$	8.9918	8.9912	8.9908	1.7706	1.7705	1.7704	2.2473	2.2473	2.2472
$N = 5$	8.9919	8.9913	8.9910	1.7707	1.7705	1.7705	3.6405	3.6404	3.6404
$N = 4$	9.2691	9.2684	9.2681	1.7707	1.7706	1.7705	3.6422	3.6422	3.6421
$N = 3$	9.2693	9.2686	9.2683	1.7711	1.7709	1.7709	9.0319	9.0319	9.0319
$N = 2$	9.3336	9.3330	9.3326	1.7716	1.7714	1.7714	9.0335	9.0335	9.0335
TBT	9.3281	9.3281	9.3281	1.7701	1.7701	1.7701	$-$[4]	$-$	$-$

1: Bending mode in the plane xz with two half waves.

2: Bending mode in the plane xy with four half waves.

3: Torsional mode.

4: Mode not provided by the theory.

Table 5: Dimensionless natural frequencies of slender cantilever beams ($l/a = 100$), modes 4 to 6.

	Mode 7[1] $\overline{\omega} \times 10^{-1}$			Mode 8[2] $\overline{\omega} \times 10^{-1}$			Mode 9[3] $\overline{\omega} \times 10^{-1}$		
FEM 3D$_{30}$	2.2940			3.4651			4.1172		
FEM 3D$_{10}$	2.2942			3.4652			4.1177		
	B2	B3	B4	B2	B3	B4	B2	B3	B4
$N = 18$	2.3252	2.3250	2.3250	3.4660	3.4656	3.4654	4.2032	4.2028	4.2027
$N = 17$	2.3252	2.3250	2.3250	3.4660	3.4656	3.4654	4.2032	4.2028	4.2027
$N = 16$	2.3253	2.3251	2.3251	3.4660	3.4656	3.4654	4.2035	4.2031	4.2030
$N = 15$	2.3253	2.3252	2.3251	3.4660	3.4656	3.4654	4.2035	4.2031	4.2030
$N = 14$	2.3363	2.3361	2.3360	3.4660	3.4656	3.4654	4.2343	4.2339	4.2338
$N = 13$	2.3363	2.3361	2.3360	3.4660	3.4656	3.4654	4.2343	4.2340	4.2338
$N = 12$	2.3367	2.3366	2.3365	3.4660	3.4656	3.4654	4.2356	4.2352	4.2351
$N = 11$	2.3368	2.3366	2.3365	3.4660	3.4656	3.4654	4.2357	4.2353	4.2351
$N = 10$	2.3570	2.3569	2.3568	3.4660	3.4656	3.4654	4.2935	4.2931	4.2929
$N = 9$	2.3571	2.3569	2.3568	3.4660	3.4656	3.4654	4.2935	4.2931	4.2930
$N = 8$	2.3668	2.3666	2.3665	3.4660	3.4656	3.4654	4.3215	4.3211	4.3209
$N = 7$	2.3668	2.3666	2.3666	3.4660	3.4656	3.4655	4.3216	4.3212	4.3211
$N = 6$	2.3997	2.3995	2.3994	3.4661	3.4656	3.4655	4.4180	4.4176	4.4175
$N = 5$	2.3998	2.3996	2.3995	3.4662	3.4658	3.4656	4.4183	4.4179	4.4177
$N = 4$	2.5676	2.5674	2.5673	3.4662	3.4658	3.4657	4.9553	4.9547	4.9546
$N = 3$	2.5677	2.5675	2.5674	3.4669	3.4665	3.4664	4.9555	4.9549	4.9548
$N = 2$	2.6097	2.6095	2.6094	3.4684	3.4680	3.4679	5.1033	5.1027	5.1025
TBT	2.6082	2.6081	2.6081	3.4654	3.4652	3.4652	5.1003	5.1000	5.1000

1: Bending mode in the plane xz with four half waves.

2: Bending mode in the plane xy with five half waves.

3: Bending mode in the plane xz with five half waves.

Table 6: Dimensionless natural frequencies of slender cantilever beams ($l/a = 100$), modes 7 to 9.

	Mode 1[1]			Mode 2[2]			Mode 3[3]		
	$\overline{\omega} \times 10$			$\overline{\omega}$			$\overline{\omega}$		
FEM 3D$_{40}$	9.0895			1.0039			2.3750		
FEM 3D$_{10}$	9.0981			1.0042			2.3761		
	B2	B3	B4	B2	B3	B4	B2	B3	B4
$N = 19$	9.3582	9.3573	9.3563	1.0042	1.0040	1.0040	2.4294	2.4292	2.4291
$N = 18$	9.4245	9.4237	9.4233	1.0042	1.0040	1.0040	2.4299	2.4298	2.4297
$N = 17$	9.4248	9.4240	9.4236	1.0042	1.0040	1.0040	2.4303	2.4301	2.4300
$N = 16$	9.4259	9.4252	9.4248	1.0042	1.0040	1.0040	2.4304	2.4302	2.4302
$N = 15$	9.4263	9.4255	9.4251	1.0042	1.0040	1.0040	2.4520	2.4518	2.4517
$N = 14$	9.5514	9.5506	9.5502	1.0042	1.0040	1.0040	2.4531	2.4529	2.4528
$N = 13$	9.5517	9.5509	9.5505	1.0042	1.0040	1.0040	2.4543	2.4541	2.4540
$N = 12$	9.5569	9.5561	9.5557	1.0042	1.0041	1.0040	2.4546	2.4544	2.4544
$N = 11$	9.5578	9.5570	9.5566	1.0042	1.0041	1.0040	2.5000	2.4998	2.4998
$N = 10$	9.7999	9.7991	9.7987	1.0042	1.0041	1.0040	2.5024	2.5022	2.5021
$N = 9$	9.8003	9.7995	9.7991	1.0042	1.0041	1.0041	2.5319	2.5317	2.5317
$N = 8$	9.9212	9.9203	9.9199	1.0042	1.0041	1.0041	2.5342	2.5340	2.5340
$N = 7$	9.9241	9.9233	9.9229	1.0043	1.0042	1.0041	2.6337	2.6335	2.6334
$N = 6$	10.358	10.358	10.357	1.0043	1.0042	1.0042	2.6376	2.6374	2.6373
$N = 5$	10.364	10.363	10.363	1.0048	1.0047	1.0046	3.9326	3.9324	3.9323
$N = 4$	13.510	13.508	13.508	1.0049	1.0048	1.0047	3.9587	3.9586	3.9585
$N = 3$	13.518	13.517	13.517	1.0076	1.0076	1.0076	9.0619	9.0618	9.0618
$N = 2$	14.742	14.741	14.740	1.0099	1.0099	1.0099	9.0855	9.0854	9.0854
TBT	14.681	14.681	14.681	1.0030	1.0029	1.0030	$-$[4]	$-$	$-$

1: Bending mode in the plane xz with one half wave.

2: Bending mode in the plane xy with one half wave.

3: Torsional mode with two half waves.

4: Mode not provided by the theory.

Table 7: Dimensionless natural frequencies of short cantilever beams ($l/a = 10$), modes 1 to 3.

	Mode 4[1]			Mode 5[2]			Mode 6[3]		
	$\overline{\omega}$			$\overline{\omega}$			$\overline{\omega}$		
FEM 3D$_{40}$	3.0472			5.9161			6.0220		
FEM 3D$_{10}$	3.0520			5.9278			6.0244		
	B2	B3	B4	B2	B3	B4	B2	B3	B4
$N = 19$	3.1540	3.1535	3.1531	6.1402	6.1389	6.1383	6.0236	6.0226	6.0223
$N = 18$	3.1805	3.1802	3.1801	6.1951	6.1940	6.1937	6.0237	6.0226	6.0223
$N = 17$	3.1809	3.1806	3.1804	6.1967	6.1955	6.1952	6.0237	6.0226	6.0223
$N = 16$	3.1814	3.1810	3.1809	6.1977	6.1965	6.1963	6.0237	6.0226	6.0223
$N = 15$	3.1818	3.1815	3.1814	6.1997	6.1985	6.1982	6.0237	6.0227	6.0224
$N = 14$	3.2328	3.2324	3.2323	6.3059	6.3047	6.3045	6.0237	6.0227	6.0224
$N = 13$	3.2332	3.2328	3.2327	6.3075	6.3064	6.3061	6.0238	6.0227	6.0224
$N = 12$	3.2353	3.2349	3.2348	6.3119	6.3108	6.3105	6.0238	6.0228	6.0225
$N = 11$	3.2365	3.2362	3.2360	6.3173	6.3161	6.3158	6.0240	6.0229	6.0226
$N = 10$	3.3382	3.3378	3.3377	6.5324	6.5312	6.5309	6.0240	6.0230	6.0227
$N = 9$	3.3387	3.3384	3.3382	6.5348	6.5336	6.5333	6.0241	6.0231	6.0228
$N = 8$	3.3909	3.3906	3.3904	6.6456	6.6445	6.6442	6.0242	6.0232	6.0229
$N = 7$	3.3948	3.3945	3.3944	6.6626	6.6614	6.6611	6.0245	6.0235	6.0232
$N = 6$	3.5921	3.5917	3.5916	7.0940	7.0927	7.0924	6.0247	6.0238	6.0235
$N = 5$	3.5991	3.5987	3.5986	7.1216	7.1203	7.1200	6.0273	6.0263	6.0261
$N = 4$	5.9410	5.9405	5.9403	12.757	12.755	12.755	6.0279	6.0270	6.0267
$N = 3$	5.9571	5.9568	5.9568	12.818	12.817	12.817	6.0431	6.0425	6.0425
$N = 2$	8.5214	8.5202	8.5200	21.540	21.536	21.536	6.0828	6.0821	6.0821
TBT	8.4916	8.4912	8.4912	21.479	21.477	21.477	6.0436	6.0433	6.0433

1: Bending mode in the plane xz with two half waves.

2: Bending mode in the plane xz with four half waves

3: Bending mode in the plane xy with two half waves.

Table 8: Dimensionless natural frequencies of short cantilever beams ($l/a = 10$), modes 4 to 6.

	Mode 7[1]			Mode 8[2]			Mode 9[3]		
	$\overline{\omega}$			$\overline{\omega}$			$\overline{\omega} \times 10^{-1}$		
FEM 3D$_{40}$	7.9914			9.0466			1.2804		
FEM 3D$_{10}$	7.9957			9.0789			1.2896		
	B2	B3	B4	B2	B3	B4	B2	B3	B4
$N = 19$	8.1367	8.1356	8.1353	9.3597	9.3565	9.3554	1.3198	1.3191	1.3187
$N = 18$	8.1400	8.1390	8.1387	9.4345	9.4316	9.4311	1.3288	1.3282	1.3281
$N = 17$	8.1408	8.1398	8.1395	9.4382	9.4353	9.4348	1.3295	1.3289	1.3288
$N = 16$	8.1419	8.1408	8.1405	9.4397	9.4368	9.4363	1.3297	1.3291	1.3290
$N = 15$	8.1961	8.1951	8.1948	9.4444	9.4415	9.4410	1.3306	1.3299	1.3299
$N = 14$	8.2024	8.2014	8.2011	9.5902	9.5873	9.5868	1.3485	1.3478	1.3477
$N = 13$	8.2056	8.2045	8.2042	9.5941	9.5912	9.5907	1.3492	1.3485	1.3485
$N = 12$	8.2073	8.2062	8.2060	9.6001	9.5972	9.5967	1.3499	1.3493	1.3492
$N = 11$	8.3221	8.3211	8.3208	9.6127	9.6098	9.6093	1.3522	1.3516	1.3515
$N = 10$	8.3366	8.3356	8.3353	9.9123	9.9093	9.9088	1.3895	1.3889	1.3888
$N = 9$	8.4116	8.4106	8.4103	9.9179	9.9150	9.9145	1.3906	1.3899	1.3898
$N = 8$	8.4260	8.4250	8.4247	10.073	10.070	10.069	1.4098	1.4092	1.4091
$N = 7$	8.6805	8.6794	8.6791	10.113	10.110	10.110	1.4174	1.4168	1.4167
$N = 6$	8.7062	8.7051	8.7048	10.732	10.729	10.728	1.4965	1.4958	1.4958
$N = 5$	12.189	12.188	12.188	10.798	10.795	10.794	1.5090	1.5082	1.5081
$N = 4$	12.382	12.381	12.381	19.625	19.621	19.620	2.6733	2.6725	2.6724
$N = 3$	27.009	27.008	27.008	19.774	19.771	19.771	2.7036	2.7028	2.7028
$N = 2$	27.281	27.280	27.280	37.603	37.592	37.592	5.5467	5.5445	5.5445
TBT	$-$[4]	$-$	$-$	37.520	37.513	37.513	5.5374	5.5357	5.5357

1: Torsional mode with three half waves.

2: Bending mode in the plane xz with five half waves.

3: Bending mode in the plane xz with six half waves.

4: Mode not provided by the theory

Table 9: Dimensionless natural frequencies of short cantilever beams ($l/a = 10$), modes 7 to 9.

	Mode 1[1]			Mode 2[2]			Mode 3[3]		
	$\overline{\omega}$			$\overline{\omega}$			$\overline{\omega} \times 10^{-1}$		
FEM 3D$_{30}$	6.4244			8.6868			1.7693		
FEM 3D$_{10}$	6.4248			8.6877			1.7694		
	B2	B3	B4	B2	B3	B4	B2	B3	B4
$N = 18$	6.4272	6.4263	6.4257	8.7721	8.7710	8.7704	1.7701	1.7699	1.7697
$N = 17$	6.4272	6.4263	6.4257	8.7721	8.7710	8.7704	1.7701	1.7699	1.7697
$N = 16$	6.4272	6.4263	6.4257	8.7723	8.7713	8.7706	1.7701	1.7699	1.7697
$N = 15$	6.4272	6.4263	6.4257	8.7723	8.7713	8.7707	1.7701	1.7699	1.7697
$N = 14$	6.4272	6.4263	6.4257	8.8014	8.8003	8.7996	1.7701	1.7699	1.7697
$N = 13$	6.4272	6.4263	6.4257	8.8014	8.8003	8.7997	1.7702	1.7699	1.7697
$N = 12$	6.4272	6.4263	6.4257	8.8025	8.8015	8.8008	1.7702	1.7699	1.7697
$N = 11$	6.4272	6.4263	6.4257	8.8026	8.8015	8.8009	1.7702	1.7699	1.7697
$N = 10$	6.4273	6.4263	6.4257	8.8559	8.8548	8.8542	1.7702	1.7699	1.7697
$N = 9$	6.4273	6.4263	6.4257	8.8559	8.8548	8.8542	1.7702	1.7699	1.7697
$N = 8$	6.4273	6.4263	6.4258	8.8813	8.8802	8.8795	1.7702	1.7699	1.7697
$N = 7$	6.4273	6.4264	6.4258	8.8814	8.8803	8.8797	1.7702	1.7699	1.7697
$N = 6$	6.4274	6.4264	6.4259	8.9663	8.9652	8.9646	1.7702	1.7699	1.7697
$N = 5$	6.4279	6.4270	6.4265	8.9665	8.9654	8.9648	1.7703	1.7701	1.7699
$N = 4$	6.4280	6.4271	6.4266	9.3809	9.3797	9.3791	1.7704	1.7701	1.7699
$N = 3$	6.4304	6.4296	6.4293	9.3814	9.3802	9.3795	1.7710	1.7708	1.7707
$N = 2$	6.4330	6.4322	6.4319	9.4806	9.4793	9.4786	1.7719	1.7717	1.7716
TBT	6.4226	6.4225	6.4225	9.4695	9.4694	9.4694	1.7691	1.7690	1.7690

1: Bending mode in the plane xy with one half wave.

2: Bending mode in the plane xz with one half wave.

3: Bending mode in the plane xy with two half waves.

Table 10: Dimensionless natural frequencies of slender clamped-clamped beams ($l/a = 100$), modes 1 to 3.

	Mode 4[1] $\overline{\omega} \times 10^{-1}$			Mode 5[2] $\overline{\omega} \times 10^{-1}$			Mode 6[3] $\overline{\omega} \times 10^{-1}$		
FEM 3D$_{30}$	2.1932			3.4645			3.9161		
FEM 3D$_{10}$	2.1936			3.4647			3.9171		
	B2	B3	B4	B2	B3	B4	B2	B3	B4
$N = 18$	2.2323	2.2320	2.2319	3.4662	3.4655	3.4652	4.0132	4.0127	4.0125
$N = 17$	2.2323	2.2320	2.2319	3.4662	3.4655	3.4652	4.0132	4.0127	4.0125
$N = 16$	2.2324	2.2321	2.2320	3.4662	3.4655	3.4652	4.0136	4.0130	4.0128
$N = 15$	2.2324	2.2321	2.2320	3.4662	3.4655	3.4652	4.0136	4.0131	4.0128
$N = 14$	2.2462	2.2459	2.2457	3.4662	3.4655	3.4652	4.0485	4.0480	4.0478
$N = 13$	2.2462	2.2459	2.2458	3.4662	3.4655	3.4652	4.0486	4.0480	4.0478
$N = 12$	2.2467	2.2465	2.2463	3.4662	3.4655	3.4652	4.0500	4.0495	4.0492
$N = 11$	2.2468	2.2465	2.2463	3.4662	3.4655	3.4652	4.0501	4.0495	4.0493
$N = 10$	2.2724	2.2721	2.2719	3.4662	3.4655	3.4652	4.1160	4.1155	4.1152
$N = 9$	2.2724	2.2721	2.2720	3.4662	3.4655	3.4652	4.1160	4.1155	4.1152
$N = 8$	2.2847	2.2844	2.2843	3.4662	3.4655	3.4652	4.1482	4.1476	4.1474
$N = 7$	2.2848	2.2845	2.2843	3.4662	3.4655	3.4652	4.1484	4.1478	4.1476
$N = 6$	2.3268	2.3265	2.3264	3.4662	3.4656	3.4653	4.2600	4.2594	4.2592
$N = 5$	2.3270	2.3267	2.3265	3.4665	3.4659	3.4656	4.2604	4.2598	4.2596
$N = 4$	2.5503	2.5499	2.5498	3.4666	3.4659	3.4656	4.9124	4.9116	4.9112
$N = 3$	2.5505	2.5501	2.5499	3.4679	3.4673	3.4671	4.9128	4.9119	4.9117
$N = 2$	2.6090	2.6086	2.6084	3.4701	3.4696	3.4694	5.1031	5.1021	5.1018
TBT	2.6059	2.6058	2.6058	3.4645	3.4643	3.4643	5.0971	5.0968	5.0968

4: Bending mode in the plane xz with two half waves.

5: Bending mode in the plane xy with three half waves.

6: Bending mode in the plane xz with three half waves.

Table 11: Dimensionless natural frequencies of slender clamped-clamped beams ($l/a = 100$), modes 4 to 6.

	Mode 7[1] $\overline{\omega} \times 10^{-1}$			Mode 8[2] $\overline{\omega} \times 10^{-1}$			Mode 9[3] $\overline{\omega} \times 10^{-1}$		
FEM 3D$_{30}$	4.0417			5.7183			5.8871		
FEM 3D$_{10}$	4.0426			5.7187			5.8887		
	B2	B3	B4	B2	B3	B4	B2	B3	B4
$N = 18$	4.1511	4.1509	4.1507	5.7213	5.7199	5.7194	6.0674	6.0665	6.0662
$N = 17$	4.1517	4.1515	4.1514	5.7213	5.7199	5.7194	6.0674	6.0666	6.0662
$N = 16$	4.1518	4.1516	4.1514	5.7213	5.7199	5.7194	6.0680	6.0672	6.0668
$N = 15$	4.1973	4.1971	4.1969	5.7213	5.7199	5.7194	6.0681	6.0672	6.0669
$N = 14$	4.1975	4.1973	4.1971	5.7213	5.7199	5.7194	6.1340	6.1332	6.1328
$N = 13$	4.2001	4.1998	4.1997	5.7213	5.7199	5.7194	6.1341	6.1332	6.1329
$N = 12$	4.2001	4.1999	4.1997	5.7213	5.7199	5.7194	6.1368	6.1359	6.1356
$N = 11$	4.2961	4.2959	4.2957	5.7213	5.7199	5.7194	6.1370	6.1361	6.1358
$N = 10$	4.2965	4.2963	4.2961	5.7213	5.7200	5.7194	6.2628	6.2619	6.2615
$N = 9$	4.3590	4.3588	4.3586	5.7213	5.7200	5.7195	6.2629	6.2620	6.2616
$N = 8$	4.3594	4.3592	4.3590	5.7213	5.7200	5.7195	6.3248	6.3239	6.3235
$N = 7$	4.5709	4.5707	4.5705	5.7214	5.7200	5.7195	6.3253	6.3244	6.3240
$N = 6$	4.5717	4.5714	4.5713	5.7214	5.7201	5.7196	6.5440	6.5430	6.5426
$N = 5$	7.3411	7.3408	7.3405	5.7219	5.7206	5.7201	6.5449	6.5439	6.5436
$N = 4$	7.3484	7.3481	7.3479	5.7220	5.7207	5.7202	7.9500	7.9484	7.9479
$N = 3$	18.072	18.072	18.072	5.7241	5.7229	5.7226	7.9508	7.9492	7.9488
$N = 2$	18.078	18.078	18.078	5.7289	5.7277	5.7274	8.4115	8.4096	8.4090
TBT	$-$[4]	$-$	$-$	5.7195	5.7189	5.7189	8.4016	8.4008	8.4008

1: Torsional mode.

2: Bending mode in the plane xy with four half waves.

3: Bending mode in the plane xz with four half waves.

4: Mode not provided by the theory.

Table 12: Dimensionless natural frequencies of slender clamped-clamped beams ($l/a = 100$), modes 7 to 9.

	Mode 1[1]			Mode 2[2]			Mode 3[3]		
	$\overline{\omega}$			$\overline{\omega}$			$\overline{\omega}$		
FEM 3D$_{30}$	2.3948			5.0720			6.0534		
FEM 3D$_{10}$	2.4008			5.0896			6.0566		
	B2	B3	B4	B2	B3	B4	B2	B3	B4
$N = 19$	2.4895	2.4894	2.4888	5.2537	5.2536	5.2521	6.0547	6.0536	6.0533
$N = 18$	2.5135	2.5133	2.5131	5.2995	5.2988	5.2985	6.0547	6.0536	6.0533
$N = 17$	2.5138	2.5135	2.5134	5.3004	5.2997	5.2994	6.0547	6.0536	6.0533
$N = 16$	2.5142	2.5139	2.5138	5.3012	5.3005	5.3003	6.0547	6.0536	6.0533
$N = 15$	2.5145	2.5143	2.5142	5.3025	5.3018	5.3016	6.0548	6.0538	6.0535
$N = 14$	2.5608	2.5606	2.5605	5.3911	5.3904	5.3901	6.0549	6.0538	6.0535
$N = 13$	2.5611	2.5608	2.5607	5.3921	5.3914	5.3912	6.0549	6.0538	6.0535
$N = 12$	2.5630	2.5628	2.5627	5.3959	5.3952	5.3949	6.0551	6.0540	6.0537
$N = 11$	2.5639	2.5637	2.5636	5.3992	5.3985	5.3983	6.0553	6.0542	6.0540
$N = 10$	2.6573	2.6570	2.6569	5.5793	5.5786	5.5784	6.0554	6.0543	6.0541
$N = 9$	2.6577	2.6575	2.6573	5.5812	5.5805	5.5803	6.0556	6.0546	6.0543
$N = 8$	2.7062	2.7059	2.7058	5.6752	5.6745	5.6743	6.0558	6.0548	6.0545
$N = 7$	2.7091	2.7088	2.7087	5.6860	5.6853	5.6851	6.0564	6.0554	6.0552
$N = 6$	2.8935	2.8932	2.8931	6.0474	6.0466	6.0464	6.0570	6.0560	6.0557
$N = 5$	2.9001	2.8999	2.8998	6.0716	6.0709	6.0708	6.0620	6.0611	6.0609
$N = 4$	5.2967	5.2963	5.2962	11.069	11.068	11.068	6.0633	6.0623	6.0621
$N = 3$	5.3170	5.3168	5.3168	11.143	11.143	11.143	6.0944	6.0939	6.0939
$N = 2$	8.5296	8.5286	8.5284	20.899	20.896	20.895	6.1571	6.1566	6.1565
TBT	8.4725	8.4724	8.4724	20.791	20.790	20.791	6.0813	6.0812	6.0812

1: Bending mode in the plane xz with one half wave.

2: Bending mode in the plane xz with two half waves.

3: Bending mode in the plane xy with one half wave.

Table 13: Dimensionless natural frequencies of short clamped-clamped beams ($l/a = 10$), modes 1 to 3.

	Mode 4[1]			Mode 5[2]			Mode 6[3]		
	$\overline{\omega}$			$\overline{\omega}$			$\overline{\omega}$		
FEM 3D$_{30}$	6.4648			8.2948			1.2096		
FEM 3D$_{10}$	6.4696			8.3320			1.2200		
	B2	B3	B4	B2	B3	B4	B2	B3	B4
$N = 19$	6.5358	6.5349	6.5346	8.5614	8.5606	8.5583	1.2432	1.2429	1.2426
$N = 18$	6.5365	6.5357	6.5354	8.6276	8.6259	8.6254	1.2514	1.2510	1.2510
$N = 17$	6.5369	6.5361	6.5358	8.6299	8.6282	8.6277	1.2518	1.2515	1.2514
$N = 16$	6.5372	6.5364	6.5361	8.6312	8.6295	8.6290	1.2520	1.2516	1.2516
$N = 15$	6.5659	6.5650	6.5648	8.6343	8.6326	8.6322	1.2526	1.2522	1.2521
$N = 14$	6.5672	6.5664	6.5662	8.7635	8.7619	8.7614	1.2687	1.2683	1.2683
$N = 13$	6.5690	6.5682	6.5679	8.7660	8.7644	8.7639	1.2692	1.2688	1.2687
$N = 12$	6.5695	6.5687	6.5685	8.7715	8.7698	8.7694	1.2699	1.2695	1.2694
$N = 11$	6.6308	6.6300	6.6297	8.7797	8.7780	8.7776	1.2714	1.2710	1.2710
$N = 10$	6.6339	6.6330	6.6328	9.0459	9.0442	9.0438	1.3051	1.3047	1.3046
$N = 9$	6.6750	6.6742	6.6739	9.0506	9.0489	9.0485	1.3060	1.3056	1.3055
$N = 8$	6.6786	6.6778	6.6776	9.1903	9.1886	9.1882	1.3237	1.3234	1.3233
$N = 7$	6.8164	6.8156	6.8154	9.2167	9.2151	9.2147	1.3288	1.3284	1.3284
$N = 6$	6.8242	6.8234	6.8233	9.7628	9.7611	9.7606	1.3993	1.3990	1.3989
$N = 5$	8.8036	8.8029	8.8027	9.8214	9.8198	9.8195	1.4104	1.4101	1.4100
$N = 4$	8.8923	8.8917	8.8916	17.759	17.757	17.756	2.4710	2.4706	2.4705
$N = 3$	18.175	18.174	18.174	17.926	17.925	17.925	2.5030	2.5027	2.5027
$N = 2$	18.293	18.293	18.293	36.374	36.368	36.367	5.3577	5.3566	5.3566
TBT	$-$[4]	$-$	$-$	36.234	36.232	36.232	5.3427	5.3422	5.3423

1: Torsional mode with two half waves.

2: Bending mode in the plane xz with three half waves.

3: Bending mode in the plane xz with four half waves.

4: Mode not provided by the theory.

Table 14: Dimensionless natural frequencies of short clamped-clamped beams ($l/a = 10$), modes 4 to 6.

	Mode 7[1] $\overline{\omega} \times 10^{-1}$			Mode 8[2] $\overline{\omega} \times 10^{-1}$			Mode 9[3] $\overline{\omega} \times 10^{-1}$		
FEM 3D$_{30}$	1.4974			1.5537			1.6575		
FEM 3D$_{10}$	1.4997			1.5559			1.6830		
	B2	B3	B4	B2	B3	B4	B2	B3	B4
$N = 19$	1.5105	1.5103	1.5102	1.5540	1.5537	1.5536	1.6970	1.6964	1.6961
$N = 18$	1.5110	1.5107	1.5107	1.5540	1.5537	1.5536	1.7065	1.7058	1.7057
$N = 17$	1.5110	1.5108	1.5107	1.5540	1.5537	1.5536	1.7072	1.7064	1.7063
$N = 16$	1.5112	1.5110	1.5110	1.5540	1.5537	1.5536	1.7074	1.7066	1.7065
$N = 15$	1.5158	1.5156	1.5156	1.5540	1.5537	1.5536	1.7083	1.7076	1.7075
$N = 14$	1.5165	1.5163	1.5162	1.5540	1.5537	1.5537	1.7271	1.7263	1.7263
$N = 13$	1.5168	1.5166	1.5165	1.5540	1.5537	1.5537	1.7278	1.7271	1.7270
$N = 12$	1.5173	1.5170	1.5170	1.5541	1.5538	1.5537	1.7286	1.7279	1.7278
$N = 11$	1.5272	1.5270	1.5269	1.5541	1.5538	1.5538	1.7311	1.7304	1.7303
$N = 10$	1.5284	1.5281	1.5281	1.5542	1.5538	1.5538	1.7709	1.7701	1.7700
$N = 9$	1.5351	1.5349	1.5349	1.5542	1.5539	1.5538	1.7722	1.7715	1.7714
$N = 8$	1.5370	1.5368	1.5367	1.5543	1.5540	1.5539	1.7934	1.7927	1.7926
$N = 7$	1.5598	1.5595	1.5595	1.5544	1.5541	1.5540	1.8016	1.8009	1.8008
$N = 6$	1.5619	1.5617	1.5617	1.5545	1.5542	1.5542	1.8866	1.8859	1.8858
$N = 5$	1.8837	1.8835	1.8835	1.5556	1.5554	1.5553	1.9045	1.9038	1.9037
$N = 4$	1.8973	1.8971	1.8971	1.5561	1.5558	1.5557	3.1959	3.1951	3.1951
$N = 3$	3.6049	3.6048	3.6048	1.5631	1.5629	1.5629	3.2508	3.2502	3.2502
$N = 2$	3.6641	3.6640	3.6640	1.5894	1.5892	1.5892	7.1868	7.1849	7.1849
TBT	$-$[4]	$-$	$-$	1.5720	1.5719	1.5719	7.1720	7.1711	7.1711

1: Torsional mode with three half waves.

2: Bending mode in the plane xy with two half waves.

3: Bending mode in the plane xz with five half waves.

4: Mode not provided by the theory.

Table 15: Dimensionless natural frequencies of short clamped-clamped beams ($l/a = 10$), modes 7 to 9.